# Isomerization and Dissociation in Competition: The Two-Component Dissociation Rates of Energy Selected Methyl Formate Ions

**Oleg A. Mazyar and Tomas Baer***

*Chemistry Department, University of North Carolina at Chapel Hill, Chapel Hill, North Carolina 27599-3290*

*Received: November 12, 1997; In Final Form: January 5, 1998*

Threshold photoelectron−photoion coincidence (TPEPICO) spectroscopy has been used to investigate the unimolecular chemistry of gas-phase, energy-selected methyl formate ions, $CH_3OCHO^{\bullet+}$. The 0 K dissociation onsets for CO loss from $CH_3OCHO^{\bullet+}$ and $CH_3OCDO^{\bullet+}$ were 11.550 ± 0.020 and 11.582 ± 0.020 eV, respectively. The two-component dissociation rates are interpreted in terms of competitive fast dissociation and isomerization steps, followed by a slow dissociation from the lower energy isomer, a distonic ion with the structure $CH_2OCHOH^{\bullet+}$. Ab initio molecular orbital calculations (G2 theory) are used to obtain energies and vibrational frequencies of various ion structures and transition states. The experimental rate constants are then modeled with the RRKM statistical theory for dissociation of both $CH_3OCHO^{\bullet+}$ and $CH_2OCHOH^{\bullet+}$. From the RRKM analysis, we found that the distonic ion $CH_2OCHOH^{\bullet+}$ lies 16.2 ± 1.5 kcal/mol lower than the methyl formate ion. Rearrangement of $CH_3OCHO^{\bullet+}$ to its distonic isomer requires 15.2 ± 1.0 kcal/mol.

## Introduction

The dissociation dynamics of gas-phase, energy-selected ester ions provide some wonderful examples of how competitive isomerization and dissociation via complex reaction mechanisms can result in multicomponent dissociation rates. Two-component dissociation rates arise when an ion can dissociate rapidly via a simple bond break or isomerize via rearrangement to a lower energy structure. The dissociation rate constant from this lower energy structure will be slow because the activation energy is much higher. We have already investigated the dissociation dynamics of methyl acetate ions by photoelectron−photoion coincidence (PEPICO) time-of-flight mass spectrometry.[1,2] In that case, $CH_3O^{\bullet}$ loss proceeds by both a fast and slow rate constant, while the lower energy $CH_2OH^{\bullet}$ loss proceeds by only the slow path. The dissociation of the ethyl formate ion, an isomer of methyl acetate, is also two component. However, it fragments by a completely different mechanism via the loss of $H^{\bullet}$, $H_2O$, and HCOOH. In both methyl acetate and ethyl formate ions, the lower energy isomers that produce the slow rate constants are the enol and distonic ions in which one of the alkyl hydrogen atoms moves to the carbonyl oxygen, thereby stabilizing the ion by 10−20 kcal/mol.

The simplest of the esters is methyl formate, which has been investigated both experimentally by PEPICO[3] and theoretically by ab initio molecular orbital calculations.[4,5] The experiments of Nishimura et al.[3] indicated that this ion also dissociates by a two-component rate. However, they did not analyze the dissociation dynamics in detail. Furthermore, no detailed potential energy surface with transition, state structures and their vibrational frequencies were available at that time. We have thus undertaken a new experimental investigation of the dissociation dynamics of this ion in order to test the potential energy surfaces proposed by Heinrich et al.[4] and Smith et al.[5]

At low internal energies the methyl formate ion dissociates by a single channel via the loss of CO and the production of $CH_3OH^{\bullet+}$. This reaction, which has an activation energy of about 0.75 eV, requires considerable rearrangement, including an H atom transfer. Isotope labeling experiments showed that $CH_3O^{13}CHO^{\bullet+}$ exclusively loses $^{13}CO$ and $CH_3{}^{18}OCHO^{\bullet+}$ specifically loses $C^{16}O$.[4] Deuterium labeling studies on $CH_3OCDO$ demonstrated conclusively that the formyl D atom ends up exclusively in $CH_3OD^{\bullet+}$.[4,6] Nishimura et al.[3] measured the CO loss rates for both $CH_3OCHO^{\bullet+}$ and $CH_3OCDO^{\bullet+}$ ions and found a $k_H/k_D$ isotope effect of about 3. They also investigated the dissociation paths at higher energies where the loss of $HCO^{\bullet}$ (or $DCO^{\bullet}$) quickly dominates. Although the latter reaction appears to involve a simple cleavage of the C−O bond, it is more complex because the ionic product formed is $CH_2OH^+$ (and not the $CH_3O^+$ ion which is not stable[7−9]). Thus, the loss of $HCO^{\bullet}$ involves several isomerization steps prior to dissociation.[4]

Several ab initio MO studies of the methyl formate ion dissociation have been reported. In the most complete investigation, published by Heinrich et al.,[4] a low-energy path for the loss of CO was found at MP3/6-31G**//6-31G*+ZPE level of theory. This involves the stretching of the $CH_3O$−CHO bond which can be accomplished with relatively little energy because of the strong ion−dipole interaction between the methoxy group and the ion. In this extended state, the formyl H atom can transfer to the $CH_3O$ group, leaving an ion−dipole complex $CH_3OH^{\bullet+}\cdots CO$ which is poised to dissociate with no additional barriers. This is an important finding because the direct transfer of the formyl hydrogen to the neighboring oxygen atom of the methoxy group would require a [1,2]-hydrogen shift which is well-known to involve high barriers.[10,11]

One of the interesting aspects of the methyl formate ion dissociation is the observation of metastable ions. According to the RRKM statistical theory, slow dissociations require large activation energies. Yet, Nishimura et al.[3] found an activation energy of only 10.6 kcal/mol. (We find the somewhat higher 17 kcal/mol.) Such small activation energies lead to predicted dissociation rates well in excess of $10^{10}$ $s^{-1}$, which is 4 orders of magnitude higher than the measured rates. They thus proposed that this reaction is perhaps nonstatistical.

S1089-5639(98)00180-7 CCC: $15.00 
Published on Web 02/18/1998

In addition to the transition state leading toward CO loss products, Heinrich et al.[4] also found low-energy barriers for interconversion of the methyl formate ion to lower energy isomers, in particular the distonic ion, $CH_2OCHOH^{\bullet+}$, of which they found two rotamers. The barrier for the formation of this ion was calculated to be about 3 kcal/mol lower than the barrier for dissociation. One can thus conclude that this ion almost certainly isomerizes at least as rapidly as it dissociates directly to products. The isomerization reaction was also investigated by Smith et al.[5] using the MP4/6-311G** level of theory as well as QCISD(T)/6-311G** with ZPE correction. These workers found four distonic ion structures which are separated by relatively low transition-state barriers. The transition state connecting methyl formate ion and the various distonic ion structures was found to be only 9.8 kcal/mol, which is 5.7 kcal/mol lower than the value reported by Heinrich et al.[4] It is interesting that these two studies did agree on the relative energies of one of the distonic ions which they calculated to be −10.3 and −10.7 kcal/mol, respectively.[4,5]

## Experimental Approach

Ions are prepared by photoionization with a CW low-power VUV light source (hydrogen discharge) dispersed by a 1 m normal incidence monochromator. An electric field of 20 V/cm accelerates electrons and ions in opposite directions. Energy-analyzed (threshold) electrons are collected in delayed coincidence with ions. The electron signals are used as starts while the ion signals are used as stops for measuring the ion time-of-flight (TOF). The ion internal energy is given by $E_{int} = h\nu - IE + E_{th}$, where $h\nu$ is the photon energy, ie is the molecule's ionization energy, and $E_{th}$ is the initial thermal energy of the molecule. When the methyl formate is introduced into the chamber as a vapor, its average internal energy, including rotations, is 85 meV. However, when the gas is introduced as a seeded molecular beam, it is possible to reduce this internal energy. An added benefit of the molecular beam method of sample introduction is that the translational temperature is greatly reduced; in particular, the temperature transverse to the beam velocity is close to 0 K so that the ion TOF distribution is extremely narrow.

The ion time-of-flight region consists of a 5 cm long acceleration region with an electric field of 20 V/cm followed by a 5 mm acceleration region which accelerates the ions to 220 eV before they enter the 30 cm long drift region.

Two types of experiments were carried out. A breakdown diagram, which consists of the fractional mass analyzed ion signal as a function of the photon energy, provides a means for determining the dissociation onset. At low energies, the only ions present are the parent ions. As the energy is increased, the fragment ion intensities increase at the expense of the parent ion. In the limit of perfect energy resolution, perfect cooling of the molecule in the adiabatically expanding gas jet, and rapid dissociation when the ion energy exceeds the dissociation limit, the breakdown diagram consists of a descending step function for the parent ion and an ascending step function for the first daughter ion. However, imperfect energy resolution and thermal energy tend to broaden these steps. Still, the crossover energy (50% parent and 50% daughter ion) can be precisely interpreted and the dissociation limit extracted. The second experiment consists of the ion TOF distribution. If the dissociation is slow, ions will be produced during the course of acceleration in the 5 cm long acceleration region. When this happens, the fragment ion TOF distribution becomes asymmetric. The modeling of this asymmetry yields the ion's dissociation rate constant.

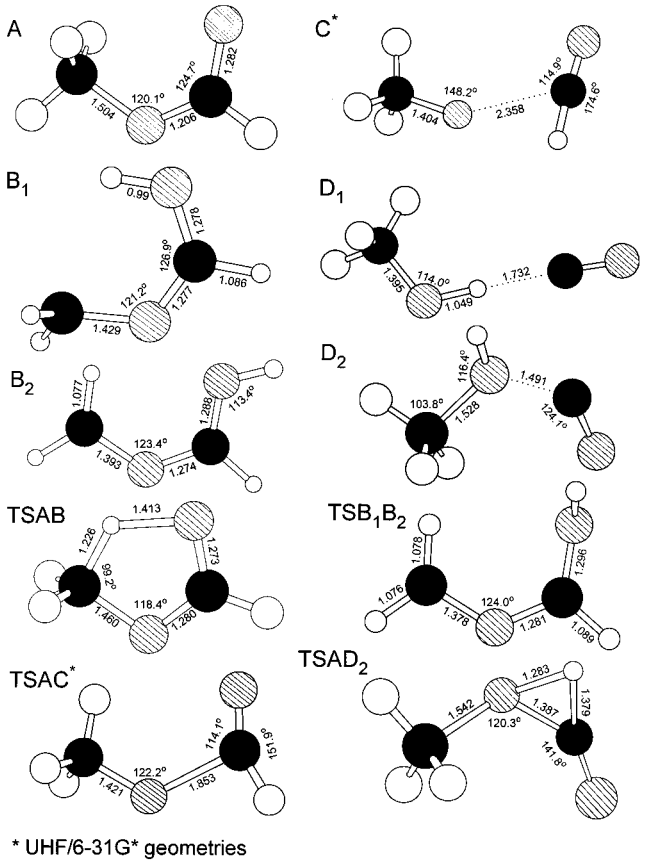


**Figure 1.** MP2(full)/6-31G* optimized geometries of the various isomers of the methyl formate radical cation and the transition states linking them. The relationship among these structures is shown in Figure 3.

## Ab Initio Molecular Orbital Calculations

To improve on calculations performed by Heinrich et al.[4] and Smith et al.,[5] we repeated their calculations using the G1[12] and G2[13−15] approaches in the GAUSSIAN 94 series of programs.[16] These two methods yielded very similar energies so that we present only the G2 results in Figure 1 and Tables 1 and 2.

To elucidate the mechanism of CO loss, we performed the geometry optimizations of the methyl formate ion with extended and frozen $CH_3O-CHO$ bond distances using the unrestricted Hartree−Fock theory of GAUSSIAN 94[16] with a split-valence 6-31G* basis set.[17] The relative energy of these structures (with respect to the ionized methyl formate) as a function of the bond distance is plotted in Figure 2. We found that the optimized geometry of these structures resembles methyl formate if the $CH_3O-CHO$ bond distance does not exceed 2.45 Å. Further elongation of this bond results in the shift of the formyl hydrogen to the methoxy oxygen and the formation of the ion−dipole complexes $CH_3OH^{\bullet+}\cdots CO$ with a large release of energy (see Figure 2).

Using optimized structures with frozen $CH_3O-CHO$ bond distances as the initial guess for further geometry optimization, we were able to locate the ion−dipole complexes $CH_3O\cdots CHO^{\bullet+}$ (C) and $CH_3OH^{\bullet+}\cdots CO$ ($D_1$) and the transition state TSAC linking the methyl formate ion (A) with the complex C. The energies for these structures are shown in Figure 3. The TSAC was confirmed at the UHF/6-31G* level by the intrinsic reaction coordinate method.[16] It is interesting that the potential energy well associated with the complex C is so shallow that it is not certain that it will remain when calculated with other basis sets.

**TABLE 1: Calculated Energies and ZPE of Ions, Transition States, and Dissociation Products**

| species | ZPE(H),[a] HF/6-31g*, hartrees | ZPE(D),[a] HF/6-31g*, hartrees | G2(H), hartrees | $E_{rel}$(H), G2, kcal/mol | $E_{rel}$(D), G2, kcal/mol |
|---|---|---|---|---|---|
| A | 0.058 870 5 | 0.055 774 5 | −228.328 902 4 | 0.00 | 0.00 |
| $B_1$ | 0.058 039 3 | 0.054 800 8 | −228.348 625 0 | −12.38 | −12.47 |
| $B_2$ | 0.057 959 8 | 0.054 753 0 | −228.356 499 2 | −17.32 | −17.39 |
| C | 0.054 062 0 | 0.051 308 0 | −228.312 142 8 | 10.52 | 10.73 |
| $D_1$ | 0.054 024 1 | 0.051 105 0 | −228.329 617 7 | −0.45 | −0.34 |
| $D_2$ | 0.057 611 6 | 0.054 435 2 | −228.322 586 8 | 3.96 | 3.91 |
| TSAC | 0.054 896 4 | 0.051 978 0 | −228.309 536 9 | 12.15 | 12.26 |
| $TSAD_2$ | 0.051 429 0 | 0.049 853 1 | −228.259 494 8 | 43.56 | 44.51 |
| TSAB | 0.054 459 6 | 0.051 303 3 | −228.313 437 6 | 9.70 | 9.67 |
| $TSB_1B_2$ | 0.055 663 1 | 0.052 480 0 | −228.336 348 2 | −4.67 | −4.73 |
| CO | 0.004 960 0 | | −113.177 498 5 | | |
| $CH_3OH^{\bullet+}$ | 0.046 411 0 | | −115.132 088 4 | | |
| $CH_3OD^{\bullet+}$ | | 0.043 595 0 | | | |
| $CH_3OH^{\bullet+}$ + CO | | | | 12.12 | |
| $CH_3OD^{\bullet+}$ + CO | | | | | 12.30 |

[a] Scaled by 0.8929.

**TABLE 2: Vibrational Harmonic Frequencies ($cm^{-1}$) Used in This Study[a]**

| | |
|---|---|
| | Methyl Formate |
| A | 85, 226, 334, 623, 753, 1021, 1134, 1152, 1190, 1357, 1413, 1433, 1451, 1619, 2933, 3005, 3040, 3073 |
| $B_1$ | 34, 265, 304, 668, 683, 799, 882, 1071, 1119, 1149, 1356, 1378, 1410, 1627, 2994, 3088, 3141, 3511 |
| $B_2$ | 144, 281, 357, 542, 617, 696, 873, 1051, 1103, 1178, 1327, 1391, 1413, 1664, 3021, 3057, 3180, 3546 |
| TSAB | 2498i, 304, 516, 574, 853, 924, 1048, 1103, 1126, 1126, 1231, 1349, 1408, 1553, 1665, 2974, 3061, 3092 |
| $TSB_1B_2$ | 648i, 185, 280, 382, 527, 709, 830, 872, 1085, 1141, 1280, 1376, 1396, 1612, 3017, 3059, 3178, 3505 |
| TSAC | 145i, 69, 87, 199, 495, 838, 895, 1025, 1062, 1150, 1379, 1421, 1448, 2075, 2879, 2962, 3004, 3110 |
| $TSAD_2$ | 1962i, 92, 151, 254, 582, 599, 694, 797, 1094, 1106, 1391, 1416, 1426, 1780, 2092, 2942, 3071, 3089 |
| | Methyl Formate-$d_1$ |
| A | 85, 225, 298, 614, 729, 860, 937, 1133, 1159, 1276, 1405, 1433, 1451, 1604, 2229, 2933, 3040, 3073 |
| $B_1$ | 34, 265, 280, 662, 677, 798, 846, 890, 1014, 1113, 1176, 1349, 1389, 1615, 2302, 2994, 3141, 3511 |
| $B_2$ | 144, 280, 325, 541, 615, 688, 839, 877, 1007, 1121, 1191, 1341, 1395, 1646, 2278, 3021, 3180, 3546 |
| TSAB | 2497i, 290, 485, 570, 835, 866, 876, 986, 1103, 1123, 1126, 1313, 1400, 1535, 1663, 2284, 2974, 3092 |
| $TSB_1B_2$ | 640i, 184, 280, 350, 527, 699, 760, 838, 982, 1039, 1139, 1276, 1388, 1603, 2273, 3017, 3178, 3505 |
| TSAC | 145i, 69, 80, 199, 483, 731, 734, 899, 1022, 1147, 1379, 1421, 1448, 1879, 2482, 2879, 2962, 3004 |
| $TSAD_2$ | 1440i, 92, 149, 241, 540, 588, 625, 764, 1089, 1103, 1309, 1400, 1416, 1426, 2040, 2942, 3071, 3089 |

[a] Scaled by 0.8929 HF/6-31g* frequencies. Transition-state imaginary frequencies denoted i.

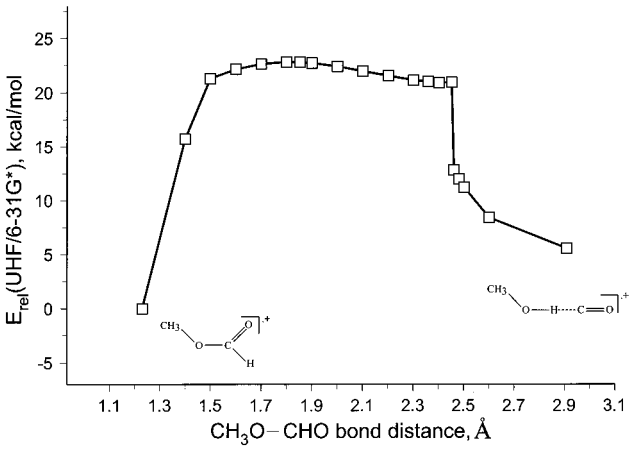


**Figure 2.** Calculated reaction path for the isomerization of the ionized methyl formate, A, to the $CH_3OH^{\bullet+}\cdots CO$ ion−dipole complex, $D_1$, using UHF/6-31G* theory. The G2 calculations reduce the rearrangement barrier from 22.8 to 12.15 kcal/mol.

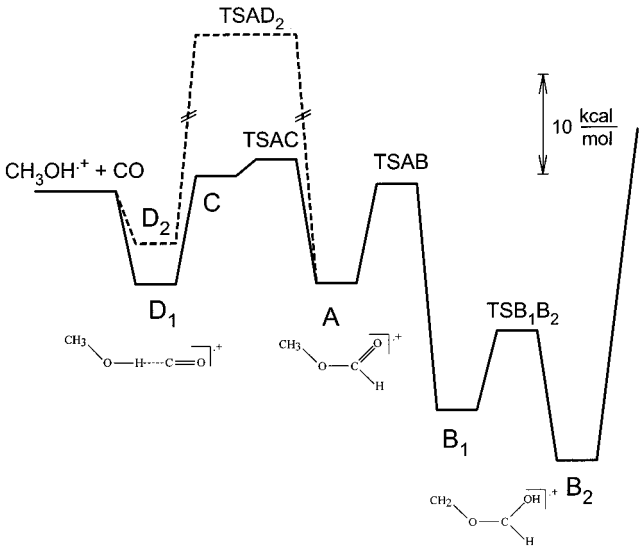


**Figure 3.** Hypersurface for rearrangement and dissociation reactions of the methyl formate ion. These G2 energies are drawn to scale except for the $TSAD_2$ which has been lowered to fit on the figure.

Unfortunately, we were not successful in finding the transition state that connects complexes C and $D_1$, but according to the results of our ab initio MO calculations on the structures with frozen $CH_3O-CHO$ bond distances (see Figure 2), the proton migration to the methoxy oxygen in the rearrangement of C to $D_1$ occurs without a detectable energy barrier. Therefore, TSAC determines the energy cost of the isomerization of the ionized methyl formate to the $CH_3OH^{\bullet+}\cdots CO$ ion−dipole complex. It should be noted that the conclusion that the hydrogen migration is not a rate-limiting step in the mechanism of CO loss is consistent with the results of our measurements of dissociative photoionization limit for the methyl formate and methyl formate-$d_1$ described below.

The G2 energy of the TSAC relative to isomer A was found to be 12.15 kcal/mol, which is considerably lower than the value of 18.8 kcal/mol proposed by Heinrich et al.[4] for the lowest energy TS for producing the $CH_3OH^{\bullet+}\cdots CO$ ion−dipole

complex. However, the geometry of the Heinrich structure is not identical with our TSAC. It is interesting that our ab initio MO calculations performed using the unrestricted Hartree−Fock theory with 6-31G* basis set yielded the relative energy of the TSAC of 22.8 kcal/mol (see Figure 2).

We have also found the transition state $TSAD_2$ for the simple [1,2]-formyl H-shift linking isomer A with the higher energy conformer $D_2$ of the complex $CH_3OH^{\bullet+}\cdots CO$ (see Figure 1). As expected, the relative energy of this transition state (43.56 kcal/mol) is too high to be involved in this reaction.[10,11] If $TSAD_2$ were involved in the mechanism of the methyl formate ion dissociation, the rearrangement of A to $D_2$ would have to proceed via tunneling of the hydrogen atom trough the very high energy barrier.

As pointed out in the Introduction, Smith et al.[5] had found four different structures for the distonic ion, $CH_2OCHOH^{\bullet+}$, but had reported high-level energies for only two of them. We have also concentrated on just two of these isomers which are shown in Figure 1 as $B_1$ and $B_2$. Our G2 energies, shown in Table 1, are slightly lower than those reported by Smith et al.[5] The relative energies of the distonic ion conformers $B_1$ and $B_2$ and the transition state $TSB_1B_2$ separating them with respect to the ionized methyl formate A were found to be lower by ∼2 kcal/mol than those calculated by Smith et al.,[5] while the G2 barrier height for the isomerization of A to $B_1$ of 9.7 kcal/mol is very close to the value of 9.8 kcal/mol reported by Smith et al.[5] (see Table 1).

Table 1 also shows the results of the G2 calculations for the analogous structures for the methyl formate-$d_1$, which differ from those of the normal methyl formate ion only by the zero-point energy difference.

To estimate the error of the G2 ab initio MO calculations, calculated relative energies of the reaction products $CH_3OH^{\bullet+}$ and CO were compared with the experimental values. The difference between calculated relative energy of the products of 12.1 kcal/mol and the 0 K value of 10.0 kcal/mol based on the experimental heats of formation of these species[18] shows that the range of possible errors in calculations of the relative energies is ±2−3 kcal/mol.

The summary of the results of the G2 ab initio MO calculations and the relationship between the different methyl formate ion isomers and transition states is shown in Figure 3. To model the dissociation rates with RRKM theory, it is helpful to consider the essential features of this potential energy surface (PES). The $D_1$ potential well is not very deep so that the lifetime of the ion in this conformation will be very short. Furthermore, the CO-loss rate constant from this well is much higher than the back-reaction because the activation energy is less and because it involves a loose transition state. Thus, we can assume (and verify) that once the methyl formate ion rearranges to the ion−dipole complex $D_1$, it dissociates rapidly and does not revert back to the starting methyl formate ion structure. We can thus ignore this well.

The distonic ion wells however are not so easily disposed of. According to Smith et al.,[5] a total of four different distonic ion conformers have comparable energies and relatively low barriers separating them. Thus, our isomerizing ion can sample the phase space of any and all of these wells before reacting back to the methyl formate ion structure. Because the transition-state energies separating these wells are considerably lower than the transition state leading over to the distonic ions (TSAB), the four distonic ion structures must be in rapid equilibrium with each other. That is, the rates for interconversion among the distonic isomers are much faster than the return rate over the TSAB barrier. Thus, we treat these wells as being in equilibrium.

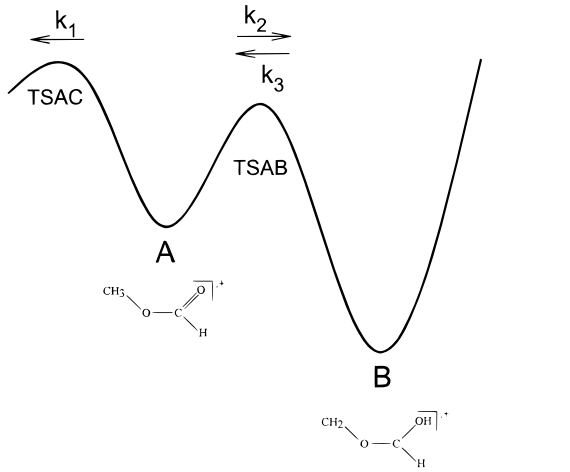


**Figure 4.** Two-well one-product model potential energy surface for the dissociation/ isomerization of the ionized methyl formate. The four distonic ion conformers are combined into a single well B.

Although the distonic ion conformers can be treated as a single well, we need to take into account their contribution to the total density of states. This is done in the following manner.[19] Suppose that isomers $B_1$, $B_2$, $B_3$, and $B_4$ have energies (relative to the methyl formate ion) of $E_1$, $E_2$, $E_3$, and $E_4$. The total density of states at an energy $E$ (again relative to the methyl formate ion) will be given by

$$\rho(E) = \rho(E - E_1) + \rho(E - E_2) + \rho(E - E_3) + \rho(E - E_4) \quad (1)$$

Thus, the deepest well (the one having the most negative energy $E_i$) will contribute the most if the vibrational frequencies of the isomers are about the same. However, it turns out that according to Table 2 the low-frequency modes of distonic ions $B_1$ and $B_2$ are very different with the most stable isomer, $B_2$, having higher low-frequency modes than isomer $B_1$. As a result, even though these two isomers are calculated to differ by as much as 5 kcal/mol in energy, their contribution to the density of states are nearly the same. Thus, it is not really possible to completely neglect these other wells from our analysis. Because the error in the calculated energies is considerable, and because small energy differences strongly affect the calculated density of states, we chose to simply replace these four wells with a single well and to multiply the density of states by a factor of 4. The energy of this composite potential energy well will then be adjusted to provide for a good fit with our experimental rate data. The resulting two-well dissociation model is shown in Figure 4.

Although our ab initio MO energies and those obtained by others agree in the general shape of the PES, it is apparent that the derived energies are not sufficiently precise to permit their use without an adjustment of ±2−3 kcal/mol in the statistical theory calculations. On the other hand, we choose to use the vibrational frequencies of the stable structures and two transition states as given by the ab initio MO calculations.

### Breakdown Diagram Analysis

Plots of fractional abundance of the parent and daughter ions as a function of photon energy for both methyl formate and deuterated methyl formate are shown in Figure 5. Data for both

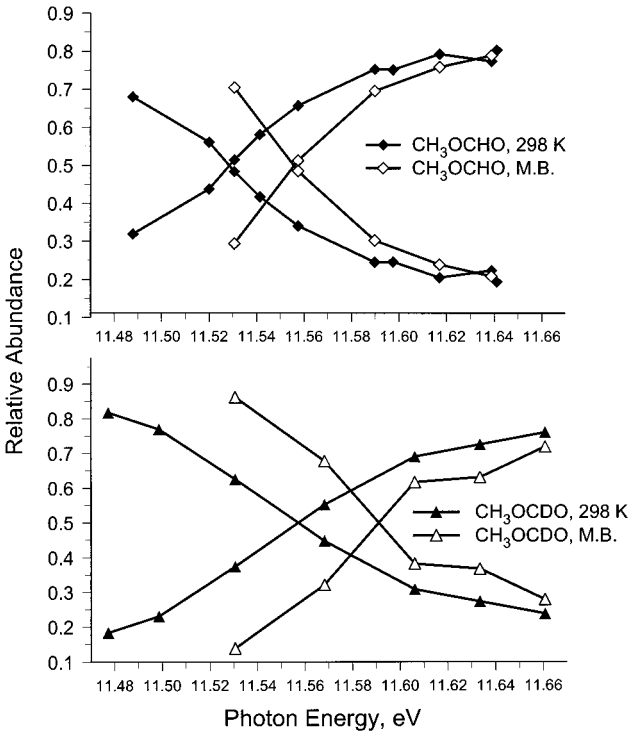


**Figure 5.** Breakdown diagrams of the methyl formate and methyl formate-$d_1$ at room temperature and under the molecular beam conditions.

the room-temperature sample and the molecular beam sample are shown. The molecular beam data were corrected for a 25% thermal background due to background gas in the experimental chamber. The molecular beam and thermal contribution were easily distinguished because the thermal data have a much broader parent ion TOF distribution (peak width of 160 ns compared to 35 ns for the molecular beam data).

The important feature in the breakdown diagrams is the crossover energy where the parent and daughter ion signals are equal. At this energy, precisely 50% of the ions have an internal energy in excess of the dissociation limit so that the dissociation limit can be determined with considerable precision. This statement is true if the minimum dissociation rate is sufficiently fast that all ions dissociate in the acceleration region. Because of the supersonic jet cooling effect, the crossover energy is shifted to higher photon energy by 28 meV as the effusive source is replaced by the molecular beam source. This is a measure of the internal energy removed during the gas-dynamic expansion.[20]

The shift in the onset depends on the nature of the transition state leading to CO loss. If this were a loose transition state located at large $CH_3OH^{\bullet+}\cdots CO$ separation, the rotational constants of the transition state would be very small so that $E^{\ddagger}_{rot} \approx 0$. That is, angular momentum in going from the molecular ion to the transition state can be conserved, while the rotational energy is not. This means that the rotational energy in the molecular ion can be used to overcome the activation barrier. On the other hand, if the transition state is tight, as is the case for most isomerization reactions, the rotational constants are nearly the same as they are in the molecular ion, so that $E^{\ddagger}_{rot} \approx E_{rot}$. In this case, rotational energy in the molecular ion does not help in overcoming the barrier because the transition-state barrier is correspondingly higher. As pointed out by Weitzel,[21] the shift in the onset of a breakdown diagram can be used to determine whether the transition state is tight or loose.

According to the ab initio MO calculations, the rotational constants of the methyl formate molecular ion and the transition state leading to dissociation, TSAC, are 20.60, 6.62, 5.18 and 21.33, 4.92, 4.10 GHz, respectively. The evolution of the rotational energy from the molecular ion to the transition state, TSAC, can be obtained by approximating the near symmetric tops by spherical tops in which the rotational constants are equal to the geometric mean of the three constants. A molecular ion having rotational energy of 309 $cm^{-1}$ ($J = 32$) would evolve into a transition state with 257 $cm^{-1}$ of rotational energy. This means that only 52 $cm^{-1}$ or 6 meV of the rotational energy (less than energy resolution) can be used to overcome the activation energy. Because a full treatment of the rotational energy in the dissociational dynamics[22] would greatly complicate the analysis without adding substantial insight, we assume that the rotational constants of the molecular ion and the transition state are the same, thereby permitting us to effectively ignore the rotational energy during the dissociation. Hence, all of the observed shift of 28 meV in the breakdown diagram can be assigned to the reduction in the vibrational energy of the molecule in the molecular beam. Since the average vibrational energy of methyl formate at 298 K is 47 meV, we see that only 19 meV of vibrational energy remains in the molecular beam sample. For the methyl formate-$d_1$, the average vibrational energy at the room temperature is 50 meV. The shift of the crossover photon energy in the breakdown diagram is 34 meV as the effusive source of $CH_3OCDO$ is replaced by the molecular beam source. Thus, the average vibrational energy of the methyl formate-$d_1$ in the molecular beam is 16 meV. This leads to calculated vibrational temperatures of 198 and 176 K for $CH_3OCHO$ and $CH_3OCDO$, respectively.

Breakdown diagrams for the warm effusive samples were used to determine the appearance energies of the product ions $CH_3OH^{\bullet+}$ and $CH_3OD^{\bullet+}$. The 0 K dissociative photoionization limit can be obtained by adding the average vibrational energy of the sample to the 298 K crossover energy. To take into account the imperfect suppression of energetic electrons by the steradiancy electron energy analyzer,[23] the 298 K crossover energy was corrected for 25 meV. In the case of methyl formate, the appearance energy of the methanol radical cation $AE_{0K}(CH_3OH^{\bullet+})$ was found to be $11.550 \pm 0.020$ eV while for the deuterated methyl formate, the $AE_{0K}(CH_3OD^{\bullet+})$ is 11.582 $\pm$ 0.020 eV. Because the dissociation rates even at threshold are relatively fast, we can equate these appearance energies with the energy of the TSAC transition state. The heat of formation of this transition state can be obtained by adding the measured appearance energy to the heat of formation of the neutral molecule:

$$\Delta H_{f(0K)}(\mathrm{TSAC}) = \mathrm{AE}_{0K}(CH_3OH^{\bullet+}) + \Delta H_{f(0K)}(CH_3OCHO) \quad (2)$$

$$\Delta H_{f(0K)}(\text{TSAC-}d_1) = \mathrm{AE}_{0K}(CH_3OD^{\bullet+}) + \Delta H_{f(0K)}(CH_3OCDO) \quad (3)$$

The 0 K heat of formation of the methyl formate ($\Delta H_{f(0K)}(CH_3OCHO) = -81.8$ kcal/mol) was determined by converting the literature value at 298 K of $-85.0$ kcal/mol[18] using experimental vibrational frequencies.[24] The 0 K heat of formation of the methyl formate-$d_1$ ($-83.7$ kcal/mol) was calculated according to the following formula:

$$\Delta H_{f(0K)}(CH_3OCDO) = \Delta H_{f(0K)}(CH_3OCHO) - \mathrm{ZPE}(CH_3OCHO) + \mathrm{ZPE}(CH_3OCDO) \quad (4)$$

**TABLE 3: Experimental Energies of Relevant Species**

| | $\Delta H_{f(0K)}$(neutral), kcal/mol | $\Delta H_{f(0K)}$(ion), kcal/mol | IE/AE, eV |
|---|---|---|---|
| $CH_3OCHO$ | −81.8[a] | | |
| $CH_3OCDO$ | −83.7[b] | | |
| $CH_3OCHO^{\bullet+}$ | | 167.4[c] | 10.815 ± 0.005[18] |
| $CH_3OCDO^{\bullet+}$ | | 165.4[d] | |
| $CH_3OH^{\bullet+}$ | | 204.6[18] | |
| $CH_3OD^{\bullet+}$ | | 202.8 | |
| CO | | −27.2[18] | |
| TSAC | | 184.5[e] | 11.550 ± 0.020[e] |
| TSAC-$d_1$ | | 183.3[e] | 11.582 ± 0.020[e] |
| TSAB | | 182.6[f] | |
| TSAB-$d_1$ | | 180.6[f] | |
| $CH_2OCHOH^{\bullet+}$ | | 151.2[f] | |
| $CH_2OCDOH^{\bullet+}$ | | 149.2[f] | |

[a] The 0 K heat of formation of methyl formate was determined by converting the literature value at 298 K of −85.0 kcal/mol[18] using experimental vibrational frequencies.[24] [b] The 0 K heat of formation of methyl formate-$d_1$ was calculated according to eq 4 using experimental vibrational frequencies for both $CH_3OCHO$ and $CH_3OCDO$.[24] [c] The 0 K heat of formation of methyl formate ion was determined by converting the literature value at 298 K of 164.4 kcal/mol[18] using the UHF/6-31G* vibrational frequencies (see Table 2). [d] The 0 K heat of formation of methyl formate-$d_1$ ion was calculated from the $\Delta H_{f(0K)}$ value for the methyl formate ion using the UHF/6-31G* vibrational frequencies for both $CH_3OCHO^{\bullet+}$ and $CH_3OCDO^{\bullet+}$. [e] The value was determined from our breakdown diagram analysis. [f] The value was determined from our RRKM analysis.

Zero-point energies were calculated using experimentally determined frequencies for methyl formate and deuterated methyl formate.[24] Thus, 0 K heats of formation of TSAC and TSAC-$d_1$ were found to be 184.5 ± 0.5 and 183.3 ± 0.5 kcal/mol, respectively. Experimental energies of all relevant species are listed in Table 3.

The 0 K heats of formation of the reaction products $CH_3OH^{\bullet+}$ and CO are 204.6 and −27.2 kcal/mol, respectively.[18] Therefore, the dissociation of both methyl formate and methyl formate-$d_1$ proceeds with a reverse activation energy barrier of about 7 kcal/mol, in contrast with the conclusion made by Nishimura et al.[3] Since the room-temperature breakdown diagram in Figure 5 is identical with that published by Nishimura et al.,[3] the discrepancy is simply the result of their improper analysis. They used the onset for observable product ion signal in their breakdown diagram which is of course much lower in room-temperature data than the crossover energy because of the Boltzmann distribution of internal energies of the methyl formate molecules.

The dissociation onset for CO loss from the deuterated sample is only 32 meV higher than that for the undeueterated sample. Is this shift a result of tunneling, or is it simply due to the difference in the zero-point energies of the two molecules? The zero-point energies of the $CH_3OCHO$ and $CH_3OCDO$ are 1.642 and 1.558 eV, respectively, while the corresponding ZPEs of the TSAC are 1.494 and 1.414 eV. Thus, the zero-point energy differences should lead to a shift of 4 meV, which is close to the experimentally observed shift. If the reaction involved tunneling through a substantial barrier, the difference in the onsets for the normal and deuterated methyl formate would be about 300 meV, far beyond the observed shift of 32 meV. The small discrepancy between the expected 4 meV and observed 32 meV shift could be due to experimental error. This conclusion is also consistent with the lowest energy transition state leading to the methanol ion product. The imaginary frequencies associated with the TSAC are only 145 $cm^{-1}$ for both normal and deuterated samples. This is clearly not consistent with tunneling as proposed by Heinrich et al.[4]

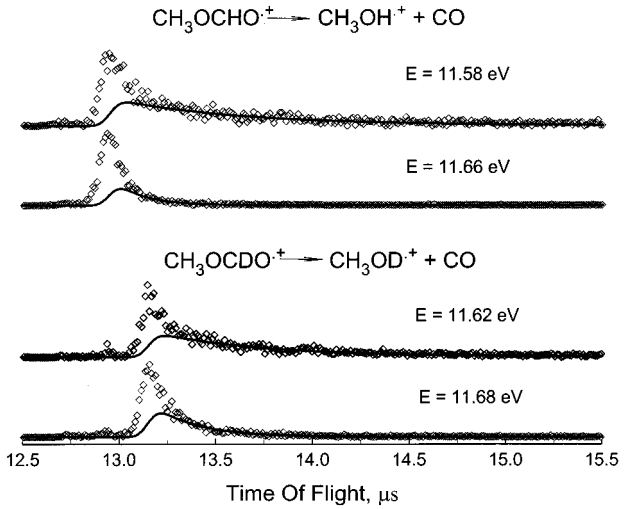


**Figure 6.** Coincidence mass spectra (diamonds) of the methyl formate and methyl formate-$d_1$ ions. Only fragment $CH_3OH^{\bullet+}$ ($CH_3OD^{\bullet+}$) ions TOF distributions are shown. The indicated photon energies were corrected for the internal energy of the molecular beam sample by adding 19 (16) meV. The solid line is a calculated TOF distribution which models the slow single-exponential decay rate.

## Rate Analysis

TOF mass spectra of methyl formate and methyl formate-$d_1$ were collected over the photon wavelength range 1063−1075 Å. Some of the TPEPICO TOF data of metastable dissociation of the $CH_3OCHO^{\bullet+}$ and $CH_3OCDO^{\bullet+}$ radical cations are presented in Figure 6 in which only fragment $CH_3OH^{\bullet+}$ and $CH_3OD^{\bullet+}$ ion TOF peaks are shown. The TOF distributions are asymmetric in this energy range because the dissociation rates are sufficiently slow so that the ions dissociate during the course of acceleration. As was pointed out by Nishimura et al.,[3] experimental TOF distributions for both $CH_3OH^{\bullet+}$ and $CH_3OD^{\bullet+}$ daughter ions could not be fitted by assuming a single rate constant of the methyl formate (methyl formate-$d_1$) ion dissociation but were found to be well reproduced with a two-component decay rate. That is, a lifetime distribution *P(t)* of the corresponding parent ion can be represented by the following formula:

$$P(t) = A \exp(-k_{fast}t) + B \exp(-k_{slow}t) \qquad (5)$$

where $k_{fast}$ and $k_{slow}$ are the dissociation rate constants and $t$ is the reaction time. This is similar to the situation encountered in three previous studies on $C_5H_{10}^{\bullet+}$, $B(OCH_3)_3^{\bullet+}$, and $CH_3COOCH_3^{\bullet+}$.[1,25,26]

The asymmetric TOF peaks of the daughter ions were used to measure the "slow" unimolecular dissociation rate constants. The rate constants of the slow component of the dissociation, $k_{slow}$, extracted from the above TOF distributions, are plotted in Figure 7 as functions of the photon energy, corrected for the internal energy of the molecular beam sample. An isotope effect of about 2 for the "slow" dissociation rates is observed.

The ratios $R$ of the "slow component" area of the fragment ion TOF distribution to the area of the "fast component" for both $CH_3OCHO^{\bullet+}$ and $CH_3OCDO^{\bullet+}$ molecular ions are shown in Figure 8. The "slow component" area was normalized by a factor of $1/[1 - \exp(-k_{slow}\tau)]$, where $\tau$ is the time it takes for the parent ion to traverse the first acceleration region, to include the "slow" product signal to $t = \infty$.

The observation of two-component dissociation rates can only be explained by the participation of two different parent ion

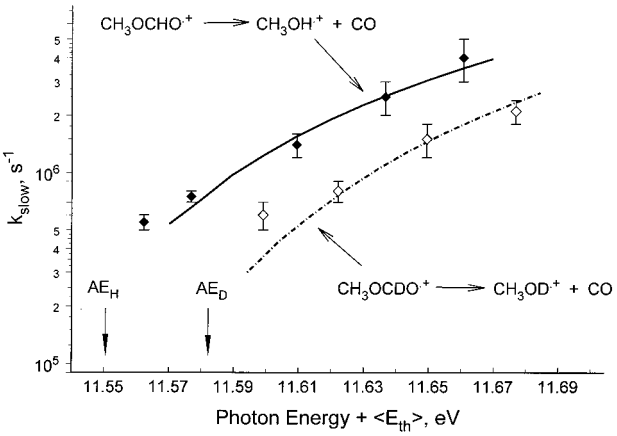


**Figure 7.** Plot of the logarithm of the experimentally observed "slow" rate constant as a function of the photon energy. The experimental data were corrected for the internal energy of the $CH_3OCHO$ molecular beam sample by adding 19 meV to the photon energy (16 meV for the $CH_3$-OCDO sample). Lines represent the best RRKM fits obtained with the two-well PES model.

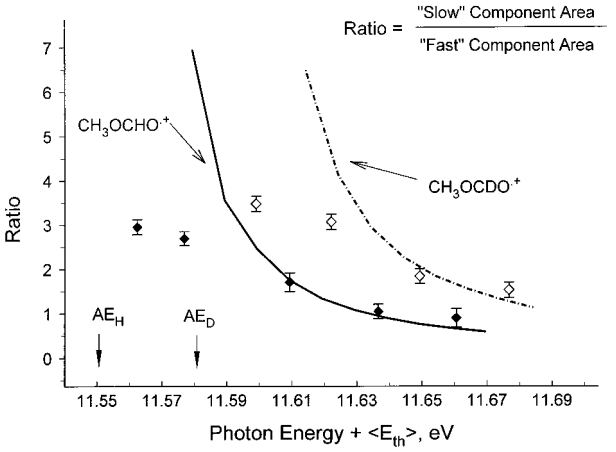


**Figure 8.** Ratio of the "slow component" area of the fragment ion TOF distribution to the "fast component" area and its best fit modeled with the two-well PES (line) vs photon energy. The experimental data were corrected for the internal energy of the $CH_3OCHO$ molecular beam sample by adding 19 meV to the photon energy (16 meV for the $CH_3$-OCDO sample).

structures in the formation of products. Thus, the present results can be described by the two-well PES shown in Figure 4. The fast component arises from the direct and fast dissociation via the transition state, TSAC. In competition with this dissociation is isomerization to the distonic ion well B. The slow rate component arises from the slow back-reaction.

The differential equations associated with this PES in Figure 4 are given by eqs 6

$$\begin{aligned} \mathrm{d[P]}/\mathrm{d}t &= k_1[\mathrm{A}] \\ \mathrm{d[A]}/\mathrm{d}t &= -(k_1 + k_2)[\mathrm{A}] + k_3[\mathrm{B}] \\ \mathrm{d[B]}/\mathrm{d}t &= k_2[\mathrm{A}] - k_3[\mathrm{B}] \end{aligned} \tag{6}$$

where P refers to the product channel.

The initial conditions are $[\mathrm{A}]_{t=0} = 1$ and $[\mathrm{B}]_{t=0} = [\mathrm{P}]_{t=0} = 0$. The solution of the system of eqs 6 for the ionized methyl formate can be represented by the following formula:

$$[\mathrm{A}](t) = \alpha_1 \exp(-k_{\mathrm{slow}}t) + \alpha_2 \exp(-k_{\mathrm{fast}}t) \tag{7}$$

For this simple two-well model, the exact expressions for $k_{\mathrm{slow}}$ and $k_{\mathrm{fast}}$ in terms of the rate constants, $k_1$, $k_2$, and $k_3$ are given by eqs 8 and 9

$$k_{\mathrm{slow}} = \frac{k_1}{k_1 + k_2} k_3 \tag{8}$$

$$k_{\mathrm{fast}} = k_1 + k_2 \tag{9}$$

The value of $k_{\mathrm{fast}}$ is too high to be measurable in our experiment, which is sensitive only to rates in the range from $5 \times 10^4$ to $1 \times 10^7$ $\mathrm{s}^{-1}$. Thus, we can evaluate only $k_{\mathrm{slow}}$. However, the ratio of the "slow" to the "fast" component can be extracted from the ion TOF data. The formula for the ratio $R$ of the areas of the "slow" to "fast" components of the fragment ion peaks is

$$R = k_2/k_1 \tag{10}$$

By substituting $k_2 = k_1 R$ into the $k_{\mathrm{slow}}$ expression, we note that

$$k_{\mathrm{slow}} = k_3/(1 + R) \tag{11}$$

which means that we can derive $k_3$ directly from the data. This is very handy as it permits us to model the well depth of the distonic ion B. However, it also means that we can only obtain the ratio of $k_2$ and $k_1$. One of these will have to be calculated by RRKM theory in order to derive the other.

We begin by evaluating $k_1$ with RRKM theory. This can be done with no adjustable parameters because the energies of the molecular ion and the transition state, TSAC, are known from the experiment, while their vibrational frequencies are known directly from our ab initio MO calculations. Once $k_1$ is determined, it is possible to obtain $k_2$ from the measured ratio, $R$. Modeling $k_2$ with RRKM theory using the energy of the isomerization transition state, TSAB, as an adjustable parameter permits us to determine the energy of TSAB. This transition-state energy cannot be taken directly from the ab initio MO calculations because the latter are not sufficiently accurate. Finally, RRKM modeling of $k_3$ using the distonic ion energy, $E_{\mathrm{B}}$, as the only adjustable parameter yields its energy. (Recall that this is just an effective energy since there are four of the distonic ion conformers.[5]) The procedure used is slightly more complicated by the fact that our ions were not perfectly vibrationally cold ($T_{\mathrm{v}} = 198$ and 176 K, respectively) so that the $k_{\mathrm{slow}}$ and $R$ in eqs 10 and 11 had to be averaged over the thermal energy distribution.

The rate constant $k_1$ was evaluated with the standard RRKM formula:

$$k_1(E) = \frac{\sigma N^{\ddagger}_{\mathrm{TSAC}}(E - E_{\mathrm{TSAC}})}{h\rho_{\mathrm{A}}(E)} \tag{12}$$

where $E$ is the methyl formate ion internal energy, $\rho_{\mathrm{A}}(E)$ is its density of states at the indicated energy, $h$ is Planck's constant, $\sigma$ is the reaction symmetry factor ($\sigma = 1$), $E_{\mathrm{TSAC}}$ is the barrier height relative to reactant A, with zero-point energies of all structures taken into account, and $N^{\ddagger}(E - E_{\mathrm{TSAC}})$ is the transition-state sum of states.

The rate constants of the isomerization processes involving hydrogen migration ($k_2$ and $k_3$) were evaluated using Miller's tunneling correction[27] to the unimolecular RRKM rate constant

$$k_2(E) = \frac{\sigma}{h\rho_A(E)}\int_{-E_{TSAB}}^{E-E_{TSAB}} K(\epsilon_t)\rho^{\ddagger}_{TSAB}(E - E_{TSAB} - \epsilon_t)\, d\epsilon_t \quad (13)$$

$$k_3(E) = \frac{\sigma}{h4\rho_B(E - E_B)}\int_{-E_{TSAB}}^{E-E_{TSAB}} K(\epsilon_t)\rho^{\ddagger}_{TSAB}(E - E_{TSAB} - \epsilon_t)\, d\epsilon_t \quad (14)$$

in which $E_B$ is the "effective" energy of the four distonic ion wells relative to the methyl formate ion A, and $\rho_B$ is the density of states of one of the distonic ion conformers, namely, $B_2$. $E_{TSAB}$ is the barrier height relative to the isomer A, $\rho^{\ddagger}_{TSAB}$ is the density of states of the transition state TSAB, $\epsilon_t$ is the translation energy in the reaction coordinate, and $K(\epsilon_t)$ is the tunneling probability modeled with an Eckart barrier.[19,28] It should be noted that tunneling in this case for both $CH_3OCHO^{\bullet+}$ and $CH_3OCDO^{\bullet+}$ involves only the H atom so that we expect no isotope effect here.

By adjusting the energy of the isomerization barrier, $E_{TSAB}$, it was possible to achieve the fit to the ratio of slow to fast components in the fragment ion's TOF distributions shown by the solid line in Figure 8. The derived barrier height was 15.2 ± 1.0 kcal/mol. The neglect of tunneling had the effect of lowering the barrier to isomerization by 1.5 kcal/mol. The agreement between calculated and measured ratio is quite good except at the lowest energy investigated. The discrepancy at low energies is probably due to imperfect modeling of the detailed form of the sample's thermal energy distribution.

Once the energy of TSAB was obtained, the effective energy of the distonic ion B could be found by fitting the energy dependence of the "slow" rate constant using eqs 11 and 14. We found that the energy of the distonic ion $CH_2OCHOH^{\bullet+}$ lies 16.2 ± 1.5 kcal/mol below the methyl formate ion energy. This fit is shown in Figure 7. The low-energy point is again not fit very well, probably for the same reason as the *R* fit in Figure 8.

It should be noted that the TSAB energy determined by RRKM analysis of the experimental data is 5.5 kcal/mol higher than the barrier calculated by G2 ab initio MO theory. A similar discrepancy is noted for the energy of TSAC. However, in the latter case, the experimental value is derived directly from the breakdown diagram with no RRKM analysis. The error in the experimental energy for TSAC is on the order of 0.5 kcal/mol.

There is a much better agreement between the effective experimental relative energy of the distonic ion isomers B and the calculated energy of the distonic ion conformer $B_2$: the theoretical value is lower only by 1.2 kcal/mol for the $CH_3OCHO^{\bullet+}$ ion.

To test the assumed model of the dissociation/ ionization mechanism of the ionized methyl formate, the PES for the methyl formate ion obtained in the result of RRKM analysis was used for modeling of the two other experimental observables: $k_{slow}$ and *R* for the deuterated methyl formate-$d_1$ ion (see Figures 7 and 8). The relative energies of the isomer B and the transition state TSAB for the methyl formate-$d_1$ ion were determined by correcting the corresponding values for $CH_3OCHO^{\bullet+}$ ion for the difference in zero-point energies. The relative energy of the TSAC was varied to fit both the "slow" rate constant and the ratio of the "slow" to "fast" component of the fragment $CH_3OD^{\bullet+}$ ion TOF distribution. We found that the best value of the relative energy of TSAC (17.7 kcal/mol with respect to isomer $CH_3OCDO^{\bullet+}$) obtained from the RRKM fit of $k_{slow}$ and *R* results in the 0 K heat of formation of TSAC of 183.1 kcal/mol, which is in an excellent agreement with the value of 183.3 ± 0.5 kcal/mol determined from the breakdown diagram analysis.

The RRKM analysis of the "slow" rate constant and the ratio of "slow" to "fast" components of the fragment ion's TOF distributions for both the methyl formate and methyl formate-$d_1$ ions was achieved with a potential energy surface that was consistent with the zero-point energy differences between these two ions. This self-consistency lends strong support of the model proposed in Figures 3 and 4.

This analysis has yielded the energies of the isomerization barrier as well as the effective energy of the distonic ion. Further tests of the mechanism would be the independent determination of all four distonic ion energies. Another test involves similar experiments with fully deuterated samples. Because the isomerization involves some tunneling through the barrier, the fully deuterated sample would exhibit a significantly less intense "slow" component in the fragment ion's TOF distribution. Furthermore, the "slow" rate constant for the deuterated sample would be less than that for the normal methyl formate ion.

**Acknowledgment.** We would like to thank the Department of Energy for continuing financial support. The authors also wish to thank the North Carolina Supercomputing Facility for the generous allotment of computing time.

## References and Notes

(1) Mazyar, O. A.; Mayer, P. M.; Baer, T. *Int. J. Mass Spectrom. Ion Processes* **1997**, *167/168*, 389.

(2) Baer, T.; Mazyar, O. A.; Keister, J. W.; Mayer, P. M. *Ber. Bunsen-Ges. Phys. Chem.* **1997**, *101*, 478.

(3) Nishimura, T.; Zha, Q.; Meisels, G. G. *J. Chem. Phys.* **1987**, *87*, 4589.

(4) Heinrich, N.; Drewello, T.; Burgers, P. C.; Morrow, J. C.; Schmidt, J.; Kulik, W.; Terlouw, J. K.; Schwarz, H. *J. Am. Chem. Soc.* **1992**, *114*, 3776.

(5) Smith, B. J.; Nguyen, M. T.; Radom, L. *J. Am. Chem. Soc.* **1992**, *114*, 1151.

(6) Van Raalte, D.; Harrison, A. G. *Can. J. Chem.* **1963**, *41*, 2054.

(7) Bouma, W. J.; Nobes, R. H.; Radom, L. *Org. Mass Spectrom.* **1982**, *17*, 315.

(8) Burgers, P. C.; Holmes, J. L. *Org. Mass Spectrom.* **1984**, *19*, 452.

(9) Schleyer, P. v. R.; Jemmis, E. D. *J. Chem. Soc., Chem. Commun.* **1978**, 190.

(10) Yates, B. F.; Bouma, W. J.; Radom, L. *J. Am. Chem. Soc.* **1987**, *109*, 2250.

(11) Yates, B. F.; Radom, L. *J. Am. Chem. Soc.* **1987**, *109*, 2910.

(12) Pople, J. A.; Head-Gordon, M.; Fox, D. J.; Raghavachari, K.; Curtiss, L. A. *J. Chem. Phys.* **1989**, *90*, 5622.

(13) Curtiss, L. A.; Raghavachari, K.; Trucks, G. W.; Pople, J. A. *J. Chem. Phys.* **1991**, *94*, 7221.

(14) Curtiss, L. A.; Raghavachari, K.; Pople, J. A. *J. Chem. Phys.* **1993**, *98*, 1293.

(15) Curtiss, L. A.; Redfern, P. C.; Smith, B. J.; Radom, L. *J. Chem. Phys.* **1996**, *104*, 5148.

(16) Frisch, M. J.; Trucks, G. W.; Schlegel, H. B.; Gill, P. M. W.; Johnson, B. G.; Robb, M. A.; Cheeseman, J. R.; Keith, T.; Petersson, G. A.; Montgomery, J. A.; Raghavachari, K.; Al-Laham, M. A.; Zakrzewski, V. G.; Ortiz, J. V.; Foresman, J. B.; Cioslowski, J.; Stefanov, B. B.; Nanayakkara, A.; Challacombe, M.; Peng, C. Y.; Ayala, P. Y.; Chen, W.; Wong, M. W.; Andres, J. L.; Replogle, E. S.; Gomperts, R.; Martin, R. L.; Fox, D. J.; Binkley, J. S.; Defrees, D. L.; Baker, J.; Stewart, J. P.; Head-Gordon, M.; Gonzalez, C.; Pople, J. P. *Gaussian 94* (*Revision D.1*); Gaussian, Inc.: Pittsburgh, PA, 1995.

(17) Hehre, W. J.; Radom, L.; Schleyer, P. v. R.; Pople, J. A. *Ab Initio Molecular Orbital Theory*; Wiley-Interscience: New York, 1986.

(18) Lias, S. G.; Bartmess, J. E.; Liebman, J. F.; Holmes, J. L.; Levin, R. D.; Mallard, W. G. Gas-Phase Ion and Neutral Thermochemistry. *J. Phys. Chem. Ref. Data* **1988**, *17* (Suppl. 1).

(19) Baer, T.; Hase, W. L. *Unimolecular Reaction Dynamics: Theory and Experiments*; Oxford: New York, 1996.
(20) Weitzel, K. M.; Booze, J. A.; Baer, T. *Chem. Phys.* **1991**, *150*, 263.
(21) Weitzel, K. M. *Chem. Phys. Lett.* **1991**, *186*, 490.
(22) Booze, J. A.; Schweinsberg, M.; Baer, T. *J. Chem. Phys.* **1993**, *99*, 4441.
(23) Baer, T.; Peatman, W. B.; Schlag, E. W. *Chem. Phys. Lett.* **1969**, *4*, 243.
(24) Shimanouchi, T. *Tables of Molecular Vibrational Frequencies*; Natl. Stand. Ref. Data Ser. (NBS) No. 39: U.S. Government Printing Office: Washington, DC, 1972.
(25) Duffy, L. M.; Keister, J. W.; Baer, T. *J. Phys. Chem.* **1995**, *99*, 17862.
(26) Mayer, P. M.; Baer, T. *J. Phys. Chem.* **1996**, *100*, 14949.
(27) Miller, W. H. *J. Am. Chem. Soc.* **1979**, *101*, 6810.
(28) Eckart, C. *Phys. Rev.* **1930**, *35*, 1303.